High-speed polygon-scanner-based wavelength-swept laser source in the telescope-less configurations with application in optical coherence tomography

S. M. R. Motaghian Nezam

California Institute of Technology, Mail Code 139-74, Pasadena, California 91125-7400, USA (rmotaghi@caltech.edu)

Received March 17, 2008; revised June 30, 2008; accepted June 30, 2008;
posted July 8, 2008 (Doc. ID 93945); published July 29, 2008

A compact high-speed tuning laser source is demonstrated in two different configurations using a polygonal mirror scanner without a telescope. It is shown that the filter configuration finesse increases by utilizing multiple reflections from the polygon facet(s) and grating illumination(s). Theoretically, the free spectral range (FSR), the instantaneous linewidth, and the finesse of each filter configuration are derived. For single grating illumination, the measured coherence length, FSR, and power were 2.8 mm, 184 nm, and 40 mW at the scanning frequency of 50 kHz, respectively. Coherence length, FSR, and power of the second laser configuration were 6.2 mm, 117 nm, and 35 mW, respectively. Finally, images of a human finger were acquired *in vivo* using two proposed swept-source configurations. © 2008 Optical Society of America

OCIS codes: 110.1650, 110.4500, 170.3880.

Wavelength-swept lasers have long been considered as optical sources in several applications including optical reflectometry, biomedical imaging, sensor interrogation, and test and measurement. In biomedical applications for optical frequency-domain imaging (OFDI), a high repetition rate of tuning is highly desirable since the sweep rate determines the imaging speed (A-line acquisition rate). In addition to high repetition rate of tuning, optical imaging applications also require wide tuning ranges to achieve a high spatial resolution, narrow instantaneous linewidths for large ranging depths, and average powers of more than ~20 mW for high sensitivity. Moreover, the finesse of the laser's spectral emission determines the ratio of the ranging depth to the resolution; to achieve high resolution and large ranging depth the laser spectrum must have a high finesse.

Two appropriate wavelength-swept laser sources have been demonstrated based on the polygonal mirror filter [1,2] and piezo-tunable Fabry–Perot filter [3]. In the polygonal mirror scheme, a telescope is used to invert the angular wavelength dispersion resulting from a diffraction grating to match the facet size and angular sweep of the polygon scanner. The resulting wavelength scan is unidirectional and has a linear dependence of wavelength upon time, characteristics that are favorable for imaging applications. In the piezo-tunable Fabry–Perot filter scheme, resonant operation of the filter results in high-speed tuning with a sinusoidal, bidirectional scan.

To increase the scanning frequency of the polygonal-mirror-based swept laser without changing the filter configuration, we may increase either the rotational speed of the polygon or the number of mirror facets. While the mechanical consideration limits the first approach, the second approach decreases the finesse of the polygon-scanning filter ($\propto$, the facet-to-facet angle of the polygon) and compromises OFDI system performance [2].

To achieve a high spatial resolution image using the polygonal-mirror-based laser source, a widely tuned swept laser has been developed to provide 145 nm at 20 kHz scan rate using two laser cavity configurations [4]. The potential challenges of this approach were laser source complexity (two telescopes and gain media), synchronization of two independent resonators, and intensity noise due to a coherent interference between two laser sweeps. Moreover, a method for increasing the finesse of a polygon scanning filter with a telescope has been reported by adding either an end reflector or a second telescope and end reflector [2]. The proposed methods can increase the finesse of the filters from ~350 to 700 and 1400 using a 72-facet polygon, respectively.

In this Letter, a compact polygon-scanning filter without a telescope in two different configurations is described that theoretically surpasses the polygon-scanning filter with one telescope in terms of finesse. First, a wavelength-swept laser using one gain medium in Littrow configuration is demonstrated with an instantaneous linewidth ~0.27 nm, wavelength sweep range of over 167.9 nm (~91% duty cycle), and average power 40 mW at 50 kHz. In the second configuration, a wavelength-swept laser is depicted with an instantaneous linewidth ~0.12 nm, wavelength sweep range of over 91.6 nm (~78% duty cycle), and average power 35 mW at 50 kHz.

The schematics of the two wavelength-scanning filter configurations are presented in Fig. 1. The tuning of the laser is accomplished by spinning of the polygon; one complete wavelength sweep is produced for each partial rotation of the polygon through an angle of $2\pi/N$, where N is the number of mirror facets, while the sweep angle of the reflected light is double the polygon's rotation angle ($\phi=2\pi/N$). The diffraction grating is placed close to the polygon scanner facet (~2 cm) to decrease beam displacement on the diffraction grating and reduce the cavity length.

0146-9592/08/151741-3/$15.00

While the first configuration depicted in Fig. 1(a) increases the free spectral range (FSR) of the filter through the Littrow illumination, the second configuration in Fig. 1(b) decreases the linewidth of the filter through multiple grating illuminations.

In Littrow configuration shown in Fig. 1(a), one facet of the polygon is used and the diffraction grating is illuminated one time. The reflected light from the polygon scanner facet illuminates the diffraction grating at Littrow's angle α and retraces the path back to the collimator. In the second configuration shown in Fig. 1(b), two facets of the polygon are used simultaneously and the diffraction grating is illuminated three times to decrease the instantaneous linewidth of the swept laser source. The reflected light from the polygon scanner facet illuminates the diffraction grating at angle α. The diffracted light at angle β from the grating illuminates another polygon facet and is returned to the same grating (or other grating with pitch p_2) at Littrow's angle γ before retracing the path back to the collimator. The orientation of the beam's incidence angle and the rotation direction of the polygonal mirror determine the direction of wavelength tuning. The arrangement in Fig. 1(b) produces a positive (increasing wavelength) sweep. Since the FSR of the filter is proportional to the sweep angle and the sweep angle of the reflected light from the polygon mirror is double the polygon's rotation angle in these configurations, the FSR will be twice that for the case when the light illuminates a grating and passes through a telescope and the polygon simply retroreflects the light back to the telescope [5].

Assuming there is no beam clipping, it can be shown that the FSR and the FWHM bandwidth (instantaneous linewidth) of two filter configurations are given by

$$\mathrm{FSR}_1 = 2p_1\Delta\alpha\cos\alpha_0, \tag{1}$$

$$\mathrm{FSR}_2 = p_1\Delta\alpha\frac{(\cos\alpha_0+\cos\beta_0)}{1\pm\dfrac{p_1\cos(\beta_0)}{2p_2\cos(\gamma_0)}}, \tag{2}$$

$$\delta\lambda_1 = \frac{2\sqrt{2\ln 2}\lambda_0 p_1\cos\alpha_0}{\pi W}, \tag{3}$$

$$\delta\lambda_2 = \frac{2\sqrt{\ln 2}\lambda_0 p_1\cos\alpha_0}{\pi W\left(1\pm\dfrac{p_1\cos(\beta_0)}{2p_2\cos(\gamma_0)}\right)}, \tag{4}$$

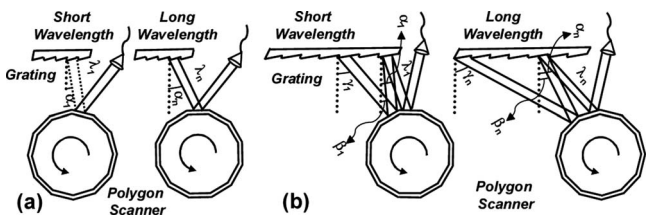

Fig. 1. (a) First and (b) second filter configurations.

where W, $\Delta\alpha(=4\pi/N)$, α_0, β_0, γ_0, p_1, and λ_0 are respectively the $1/e^2$ width of the Gaussian beam at the fiber-optic collimator, the sweep angle (range of the incident angle), the incident angle at the center wavelength, the center wavelength diffracted angle, the center wavelength Littrow's angle, grating pitch, and the center wavelength. The orientation of the beam's incidence angle and the rotation direction of the polygonal mirror determine the positive and negative signs in Eqs. (2) and (4).

As shown in Eqs. (5) and (6), the finesse of the filter is fundamentally limited by the number of mirror facets, the beam width, and the facet mirror size:

$$F_1 = \frac{\pi W\Delta\alpha}{\lambda_0\sqrt{2\ln 2}} = \frac{2\sqrt{2}\pi^2 W}{N\lambda_0\sqrt{\ln 2}}, \tag{5}$$

$$F_2 = \frac{\pi W\Delta\alpha}{2\lambda_0\sqrt{\ln 2}}\left(1+\frac{\cos\beta_0}{\cos\alpha_0}\right) = \frac{2\pi^2}{N\lambda_0\sqrt{\ln 2}}(W+D), \tag{6}$$

where D is the facet mirror size.

To have 100% duty-cycle laser tuning and avoid linewidth broadening the following necessary conditions need to be met: (1) the range of Littrow's light angle is double the polygon's rotation angle for the first configuration and the summation of the range of diffracted light angle, and the range of Littrow's light angle is double the polygon's rotation angle for the second configuration; (2) the $1/e^2$ width of the illuminated Gaussian beam on the facets is equal to or less than the facet mirror size during polygon rotation.

Figure 2(a) shows the theoretical finesse of the proposed configurations and the previously published polygon filter designs with telescope(s) [2,4,5] as a function of the polygon facets number. It is clear that the finesse of the two proposed configurations is greater than the two polygon filter designs with telescope with/without an end reflector. In addition, the second configuration achieves the same finesse as the polygon filter design with two telescopes provides [2]. For example, the finesses of the first and second configurations theoretically are 992 and 1400 at 1.3 μm using a 72-facet polygon with a facet size of 2.77 mm. In the second configuration, utilizing facets that are not directly adjacent to each other may decrease tun-

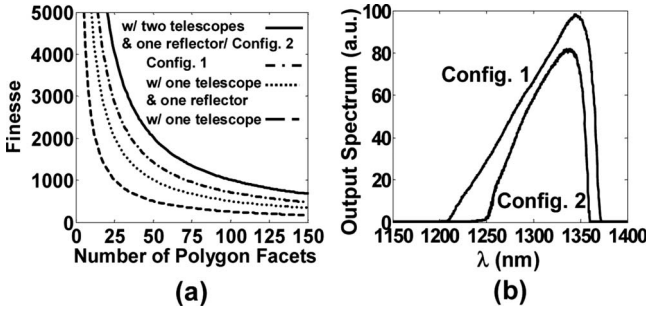

Fig. 2. (a) Finesse of several polygon filter designs with and without telescope(s) as a function of polygon facets. (b) Output spectra of the laser for the first and second filter configurations.

ing range and broaden linewidth owing to beam clipping on the polygon facet(s). In addition, grating efficiency that determines the cavity loss may decrease tuning range owing to single/multiple grating illumination(s).

The filter design configurations were constructed using a custom polygon-scanning mirror with 72 facets, corresponding to ϕ=5°, and individual facet widths of 2.77 mm. A relatively high-groove density blazed diffraction grating (1200 lines/mm) was used to decrease the linewidth. The collimator was chosen to produce a $1/e^2$ beam width of 1.9 mm to illuminate more lines on the grating. The rotational rate of the polygon could be continuously adjusted up to a maximum speed of 695 rev/s, corresponding to a filter repetition rate of 50 kHz. To test the tuning performance of this filter, a unidirectional fiber-optic resonator was constructed using a broad-bandwidth semiconductor optical amplifier (Covega BOA-2527) as a gain medium for the laser. The gain medium was coupled to the filter via an optical circulator. For the first and second configurations, the incident angles at the center wavelength were set to 50.6° and 57.5°, respectively.

Figure 2(b) shows the output spectra of the laser using two different filter configurations discussed. The edge-to-edge sweep ranges were 167.9 nm (1207.8–1375.7) and 91.6 nm (1261.9–1353.5) wide for the first and second configurations at 50 kHz scanning rate, respectively. The measured average output power of the first and second configurations were 40 and 35 mW, respectively. Using the derived equations (1) and (2), FSRs were calculated to be 184 nm and 117 nm for the first and second configurations, respectively. The calculated FSRs are in good agreement with experimental results (FSR =wavelength sweep range/duty cycle) considering the measured duty cycles 91% and 78% for the first and second configurations, respectively. The difference between the measured edge-to-edge sweep ranges and the theoretical FSR results can arise owing to the increased cavity loss caused by a multiple-facet mirror and grating illuminations. Figure 3(a) shows the oscilloscope trace of the second configuration at a repetition rate of 50 kHz. To characterize the instantaneous linewidth of the laser configurations, the point-spread function was measured using a calibrated partial reflector at various depths in the sample arm. The acquired sampled data at each depth was processed with the mapping algorithm described by Yun *et al.* [6]. The reduction in signal power with depth was ~6 dB over the entire depth span of 2.8 mm and 6.2 mm for the first and second configurations at 50 kHz, respectively. Figure 3(b) shows the processed point-spread functions over 7 mm for the second configuration. While the theoretical equations estimate linewidths of 0.07 nm for the second configuration, the difference between the measured linewidth (0.12 nm) and the theoretical result (0.07 nm) can arise owing to beam clipping and wavelength shift per round trip (0.058 nm) in the cavity at 50 kHz in the second configuration.

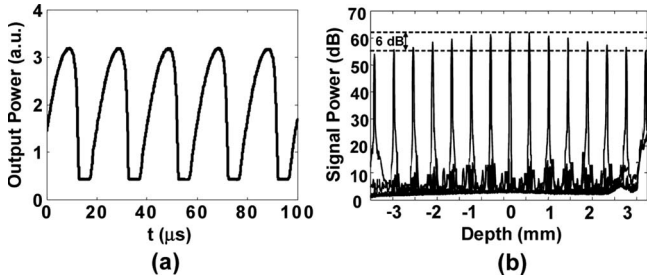

Fig. 3. (a) Oscilloscope trace of the second configuration, showing five tuning cycles at a repetition rate of 50 kHz. (b) Point-spread functions obtained at 15 different depth points after mapping to linear space. The degradation in signal power with depth is no more than 6 dB over the total depth span of 6.2 mm.

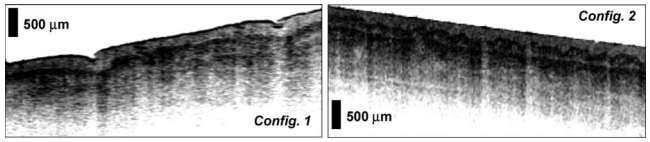

Fig. 4. Images of a human finger acquired with the OFDI system at 50 frames per second using proposed configurations.

To validate two proposed configurations, images of the portion of a finger were obtained. The laser was operated at a rate of 50 kHz so that 2000 samples could be acquired using a fixed sampling frequency of 100 MS/s. The probe, comprising a galvanometer mirror and an imaging lens, produced a 32 μm$1/e^2$ diameter focal spot on the sample with a confocal parameter of 1.1 mm. The focal point of the imaging lens was positioned in the middle of the depth range. Figure 4 depicts the portion of a finger acquired at 50 frames per second using the first and second configurations that are cropped to 520 axial ×490 transverse pixels and 340 axial ×976 transverse pixels plotted in logarithmic inverse gray scale, respectively.

The author sincerely acknowledges contributions by B. Bouma and W. Oh at Harvard Medical School and Massachusetts General Hospital.

References

1. S. H. Yun, G. J. Tearney, J. F. de Boer, N. Iftimia, and B. E. Bouma, Opt. Express **11**, 2953 (2003).
2. W. Y. Oh, S. H. Yun, G. J. Tearney, and B. E. Bouma, Opt. Lett. **30**, 3159 (2005).
3. R. Huber, M. Wojtkowski, and J. G. Fujimoto, Opt. Express **14**, 3225 (2006).
4. W. Y. Oh, S. H. Yun, G. J. Tearney, and B. E. Bouma, Photon. Technol. Lett. **17**, 678 (2005).
5. S. H. Yun, C. Boudoux, G. J. Tearney, and B. E. Bouma, Opt. Lett. **28**, 1981 (2003).
6. S. H. Yun, G. J. Tearney, J. F. de Boer, and B. E. Bouma, Opt. Express **12**, 4822 (2004).